Hard-Coupled Numerical Model of Induction Heating of Thin Profile Plates in External Magnetic Field

Ivo Dolezel[1], Bohus Ulrych[2], Jerzy Barglik[3]
[1]Czech Technical University, Faculty of Electrical Engineering,
Technicka 2, 166 27 Praha 6, Czech Republic, E-mail: dolezel@fel.cvut.cz
[2]University of West Bohemia, Faculty of Electrical Engineering,
Univerzitni 26, 306 14 Plzen, Czech Republic, E-mail: ulrych@kte.zcu.cz
[3]Silesian University of Technology, Faculty of Material Engineering and Metallurgy,
Krasinskiego 8, 40-019 Katowice, Poland, E-mail: jerzy.barglik@polsl.pl

Abstract — A new hard-coupled numerical model of induction heating of thin profile plates in external time-variable magnetic field is presented. While the currents induced in the plate are expressed in terms of electric vector *T*-potential, the distribution of temperature in it is described by the heat-transfer equation involving the effects of heat sources and sinks. All nonlinearities of the system are taken into account. The methodology is illustrated by an example of heating an axisymmetric plate spring made of phosphor bronze.

I. INTRODUCTION

Nowadays, the distribution of magnetic field in metal bodies in the process of their induction heating is mostly modeled by magnetic vector potential $\boldsymbol{A}$ [1–2]. But this approach can fail when the heated body is characterized by geometrically incommensurable dimensions. This is typical for various planar structures such as thin plates or pipes.

Consider one possible arrangement for local heating of thin nonferromagnetic plates (whose thickness δ must be smaller than the depth of penetration) depicted in Fig. 1. The field coil **3** carrying time-variable current $i(t)$ generates a time-variable magnetic field in laminated magnetic cores **2**. Magnetic flux of density $\boldsymbol{B}_{\mathrm{ext}}(\boldsymbol{r},t)$ passing between focusators **4.1** and **4.2** through the plate **1** induces in it currents of density $\boldsymbol{J}_{\mathrm{ind}}(\boldsymbol{r},t)$ that produce heat.

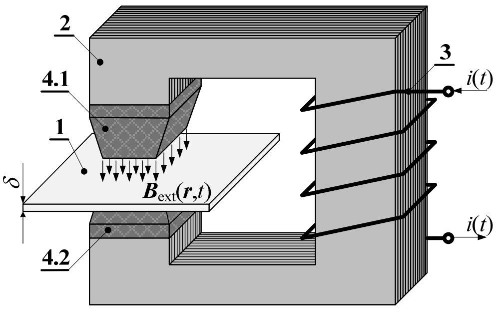

Fig. 1. Induction heating of a thin plate:
1–locally heated thin nonferromagnetic plate, **2**–laminated magnetic cores, **3**–field coil, **4.1** and **4.2**–ferromagnetic focusators

II. FORMULATION OF THE TECHNICAL PROBLEM

Modeled is induction heating of an axisymmetric profile plate spring before its annealing. The spring is made of phosphor bronze and its shape is depicted in Fig. 2. As its thickness δ is very small (usually $\delta \le 1\,\mathrm{mm}$), we can suppose that *no physical quantity varies along it*.

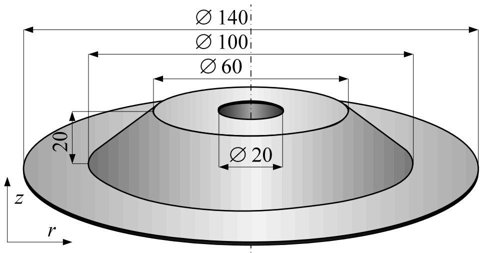

Fig. 2. Considered profile plate spring (dimensions in mm)

The spring is heated in time variable external magnetic field $\boldsymbol{B}_{\mathrm{ext}}$ that is supposed to be parallel with the z-axis (so that $\boldsymbol{B}_{\mathrm{ext}}(\boldsymbol{r},z) = \mathbf{k}\,B_{z,\mathrm{ext}}(r,z)$, $\mathbf{k}$ being the unit vector in the z-direction). This is realized by appropriately shaped focusators **4.1** and **4.2** (the upper one being fixed on a movable part of magnetic core **2**); an example is in Fig. 3.

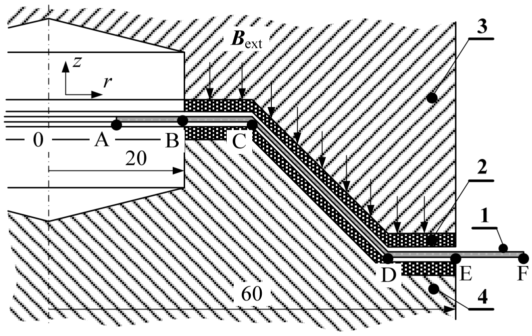

Fig. 3. Arrangement of the heated spring between the focusators:
1–heated plate spring, **2**–glass wool (thermal insulation), **3**–movable upper focusator, **4**-lower focusator

The task is to find the distribution of volumetric Joule losses in the spring and time evolution of its temperature.

III. MATHEMATICAL MODEL

The density $\boldsymbol{J}_{\mathrm{ind}}$ of currents induced in the plate follows from the relation (the second Maxwell equation)

$$\mathrm{curl}\,\boldsymbol{E} = \mathrm{curl}\left(\frac{\boldsymbol{J}_{\mathrm{ind}}}{\gamma_{\mathrm{el}}}\right) = -\frac{\partial \boldsymbol{B}}{\partial t} = -\frac{\partial\left(\boldsymbol{B}_{\mathrm{ext}} + \boldsymbol{B}_{\mathrm{add}}\right)}{\partial t}, \quad (1)$$

where $\boldsymbol{B}_{\mathrm{add}}$ is an additional current density produced by the induced currents. Introduce now electric vector potential $\boldsymbol{T}$ by the relation [3], [4]

$$\boldsymbol{J}_{\mathrm{ind}} = -\mathrm{curl}\,\boldsymbol{T}\,. \quad (2)$$

After substitution of (2) to (1) we obtain

$$\operatorname{curl}\left(\frac{1}{\gamma_{\text{el}}}\operatorname{curl}\boldsymbol{T}\right)=\frac{\partial \boldsymbol{B}_{\text{ext}}}{\partial t}+\frac{\partial \boldsymbol{B}_{\text{add}}}{\partial t}. \tag{3}$$

Applying the first Maxwell equation to the plate (the time variations are considered sufficiently low, so that the displacement currents can be neglected), we obtain

$$\operatorname{curl}\left(\frac{1}{\mu_0}\boldsymbol{B}_{\text{add}}\right)=\boldsymbol{J}_{\text{ind}} \tag{4}$$

and, substituting from (2), we have

$$\operatorname{curl}\left(\frac{1}{\mu_0}\boldsymbol{B}_{\text{add}}\right)=-\operatorname{curl}\boldsymbol{T}. \tag{5}$$

Hence, generally, $\boldsymbol{T}=-\boldsymbol{B}_{\text{add}}/\mu_0-\operatorname{grad}\psi$, where ψ is an arbitrary scalar function. But in our case $\boldsymbol{T}$ represents the electric vector potential only produced by the induced magnetic flux density $\boldsymbol{B}_{\text{add}}$. That is why $\operatorname{grad}\psi=\boldsymbol{0}$ and

$$\boldsymbol{B}_{\text{add}}=-\mu_0\boldsymbol{T}. \tag{6}$$

Inserting this result to (3) immediately provides the basic nonlinear parabolic equation for $\boldsymbol{T}$ in the form

$$\operatorname{curl}\left(\frac{1}{\gamma_{\text{el}}}\operatorname{curl}\boldsymbol{T}\right)+\mu_0\frac{\partial \boldsymbol{T}}{\partial t}=\frac{\partial \boldsymbol{B}_{\text{ext}}}{\partial t}, \tag{7}$$

whose right-hand side is known.

The initial condition is $\boldsymbol{T}(\Omega_1,t=0)=\boldsymbol{0}$. The boundary condition follows from the fact that the current density in the direction of any outward normal to the spring vanishes. In other words $\gamma_{\text{el}}\cdot\partial\boldsymbol{T}(\Gamma,t)/\partial\tau=0\Rightarrow\boldsymbol{T}(\Gamma,t)=\boldsymbol{C}$ ($\boldsymbol{\tau}$ denoting the tangent, Γ the boundary), where $\boldsymbol{C}$ is a constant vector. In order to preserve the consistency with the above initial condition, we immediately obtain $\boldsymbol{C}=\boldsymbol{0}$.

The temperature field produced by the heat losses w_{J} is described by the modified heat-transfer equation [5]

$$\operatorname{div}(\lambda\operatorname{grad}T)=\rho c\frac{\partial T}{\partial t}-w_{\text{J}}+ \\ +\frac{1}{\delta}\left[\left(\alpha_{\text{c,up}}+\alpha_{\text{c,dn}}\right)\left(T-T_{\text{ext,c}}\right)+2\varepsilon_{\text{SB}}C_{\text{r}}\left(T^4-T_{\text{ext,r}}^4\right)\right], \tag{8}$$

where T is the temperature, λ is the thermal conductivity, ρ is the specific mass, c is the specific heat,. ε_{SB} is the Stefan-Boltzmann constant, C_{r} is the coefficient of emissivity, $T_{\text{ext,c}}$, $T_{\text{ext,r}}$ are the distant temperatures for simulation of convection and radiation and, finally, $\alpha_{\text{c,up}}$ and $\alpha_{\text{c,dn}}$ are the coefficients of convective heat transfer along the upper and lower sides of the spring. But in the space between the focusators, the process of heating is considered adiabatic.

IV. ILLUSTRATIVE EXAMPLE

The basic dimensions of the plate spring are given in Figs. 2 and 3, its thickness $\delta=1\,\text{mm}$. Other input parameters: $B(r,t)=B_0\sin(\omega t)$, $B_0=1\,\text{T}$, $f=10\,\text{kHz}$, $C_{\text{r}}=0.5$, $\alpha_{\text{c,up}}=20\,\text{W/m}^2\text{K}$, $\alpha_{\text{c,dn}}=5\,\text{W/m}^2\text{K}$, $T_{\text{ext,c}}=T_{\text{ext,r}}=20\,°\text{C}$. Parameters γ_{el}, λ, ρc of the phosphor bronze (94 % Cu, about 5 % Sn, a small amount of Zn) are functions of temperature (function $\gamma_{\text{el}}(T)$ being depicted in Fig. 4).

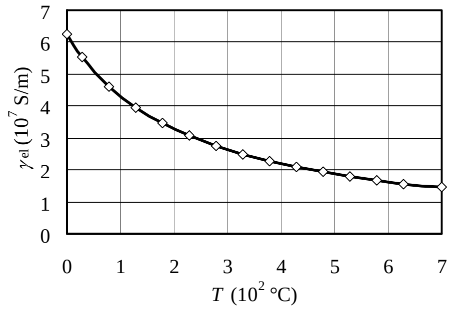

Fig. 4. Dependence $\gamma_{\text{el}}(T)$ for phosphor bronze

Computations were realized in the hard-coupled formulation, by a code developed by the authors. Carefully were tested both convergence and stability of the results. Figure 5 shows the distribution of the temperature along the surface of the spring at several levels of time.

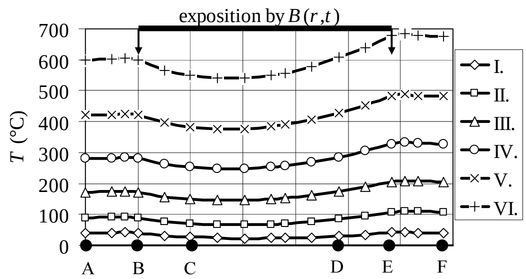

Fig. 5. Heating of the spring in at several time levels (I. $t=1$ s, II. $t=5$ s, III. $t=10$ s, IV. $t=15$ s, V. $t=20$ s, VI. $t=25$ s), the points A, B, C, D, E, F being marked in Fig. 3

The highest temperatures are at points B and E identical with the internal and external edges of the focusators (and also the places of highest changes of the electric vector potential and values of induced currents and Joule losses). The acceleration of heating in time is caused by fast increase of specific resistance of the phosphor bronze (Fig. 4), while the induced currents decrease rather slowly.

V. ACKNOWLEDGMENT

The financial support of the Grant Agency of the Czech Republic (project No. 102/09/1305) and Grant Agency of the Academy of Sciences of the Czech Republic (project No. IAA100760702) is gratefully acknowledged.

VI. REFERENCES

[1] V. I. Rudnev, D. Loveless, R. Cook, and M. Black, *Handbook of Induction Heating*, CRC Press, New York, 2002.

[2] E. Rapoport and Y. Pleshivtseva, *Optimal Control of Induction Heating Processes*, CRC Press, Boca Raton, FL, USA, 2007.

[3] D. Albertz and G. Henneberger, "Calculation of 3D eddy current fields using both electric and magnetic vector potential in conducting regions," *IEEE Trans. on Magn.*, vol. 34, no.5, pp. 2644–2647, 1998.

[4] R. Albanese and G. Rubinacci, "Treatment of multiply connected regions in two-component electric vector potential formulations" *IEEE Trans. on Magn.*, vol. 26, no.2, pp. 650–653, 1990.

[5] J. P. Holman, *Heat Transfer*, McGrawHill, 2002.